IN-07
14439
P12

NASA Technical Memorandum 103757

Advanced Ice Protection Systems Test in the NASA Lewis Icing Research Tunnel

Thomas H. Bond and Jaiwon Shin
National Aeronautics and Space Administration
Lewis Research Center
Cleveland, Ohio

and

Geert A. Mesander
United States Air Force
Oklahoma City Air Logistics Center
Tinker Air Force Base, Oklahoma

Prepared for the
47th Annual Forum and Technology Display
sponsored by the American Helicopter Society
Phoenix, Arizona, May 6–8, 1991

NASA

(NASA-TM-103757) ADVANCED ICE PROTECTION SYSTEMS TEST IN THE NASA LEWIS ICING RESEARCH TUNNEL (NASA) 12 p CSCL 21E

N91-23183

Unclas
G3/07 0014439

ADVANCED ICE PROTECTION SYSTEMS TEST IN THE NASA LEWIS ICING RESEARCH TUNNEL

Thomas H. Bond and Jaiwon Shin
National Aeronautics and Space Administration
Lewis Research Center
Cleveland, Ohio

Geert A. Mesander
United States Air Force
Oklahoma City Air Logistics Center
Tinker Air Force Base, Oklahoma

ABSTRACT

Tests of eight different deicing systems based on variations of three different technologies were conducted in the NASA Lewis Research Center Icing Research Tunnel in June and July of 1990. Six companies participated in this joint United States Air Force/NASA ice protection technology program. The deicing systems used pneumatic, eddy current repulsive, and electro-expulsive means to shed ice. The tests were conducted on a 1.83 m (6 ft) span, 0.53 m (21 in.) chord NACA 0012 airfoil operated at a 4° angle-of-attack. The models were tested at two temperatures: a glaze condition at -3.9 °C and a rime condition at -17.2 °C. The systems were tested through a range of icing spray times and cycling rates. Characterization of the deicers was accomplished by monitoring power consumption, ice shed particle size, and residual ice. High speed video motion analysis was performed to quantify ice particle size.

INTRODUCTION

Throughout the last decade there have been a number of new developments in ice protection technology. Innovative deicing systems have been designed and tested based on electro-mechanical, pneumatic-mechanical, thermal, and conventional pneumatic techniques. As these systems have matured in development the aircraft industry has shown increasing interest in them as alternate choices to the current technology. With the advent of the increased use of turbofan engines on modern aircraft the engine core flow has decreased substantially, causing concern about the operation of engine bleed air equipment, i.e., hot bleed air anti-icing systems. The high cost in electrical power has always been an issue in restricting the application of electrically heated (thermal) anti-icers. The advances in new low power ice protection designs may provide opportunities to overcome the above limitations.

Until this test, there had been no broad based study to define the capabilities of these new deicing systems. The United States Air Force (USAF) Oklahoma City Air Logistics Center and NASA Lewis Research Center initiated a program to test low power ice protection systems to assess the current state-of-the-art of these technologies. After solicitation for companies to test in the Icing Research Tunnel (IRT) was announced, a strong response from industry supported the need to identify the capabilities of these new ice protection systems. Six companies with a total of eight different systems (Table 1) agreed to test their hardware; however, this did not represent all the new technologies. The systems ranged in developmental maturation from limited ice tunnel testing to the near certification stage, with some having been flight tested in icing conditions. NASA Lewis provided airfoil leading edges to a majority of the entrants for mounting their deicers (two systems elected to construct their own leading edge hardware); one common trailing edge was installed in the tunnel. It was decided to use high speed videography, system power monitoring instrumentatio n, and measurement of residual ice to quantify system performance. These measuring techniques, along with a range of spray times, cloud conditions, and systems check-out yielded a test matrix of 41 hours of testing per entrant.

This paper will present an overview of the systems tested, discuss the test equipment, outline the test procedures, and report typical results representative of the reduced data.

TABLE 1. - TEST PARTICIPANTS (IN ORDER OF IRT TESTING)

Company	System	
BF Goodrich De-Icing Systems	Pneumatic Impulse Ice Protection	(PIIP)
BF Goodrich De-Icing Systems	Small Tube Pneumatic	(STP)
Rohr Industries, Inc.	Electro-Impulse De-Icing	(EIDI)
Electroimpact, Inc.	Eddy Current De-Icing Strip	(EDS)
BF Goordich De-Icing Systems	Electro-Mechanical System	(EMS)
Advance Concepts De-Icing Company	Electro-Impulse De-Icing	(EIDI)
Garrett Canada	Electro-Impulse De-Icing	(EIDI)
Dataproducts New England, Inc.	Electro-Expulsive De-Icing System	(EEDS)

TECHNICAL APPROACH

To facilitate equal testing of all the systems, a generic airfoil with a relatively mild leading edge radius was chosen. This eliminated any geometry sensitive issues in regard to both hardware installation and operation for the range of systems tested. The airfoil was set at an angle-of-attack to provide air loads similar to flight conditions to assist in ice removal. Two cloud conditions were chosen: a near freezing glaze ice, and a hard rime ice. Both reflect ice accretions that have historically been the hardest to remove. Once the above physical criteria and cloud conditions were set, the actual characterization of system performance was addressed. The key parameters focused on were power, residual ice, and quantification of shed ice particle size. Deicer boot weight was also measured. Power was monitored through a watt-meter. The companies provided the voltage and capacitance to NASA for capacitor bank storage supplies, and their electrical current discharge traces were recorded on a digital storage scope. At the end of a test point residual ice was documented both pictorially and quantitatively. Shed ice information was captured on high speed videography and high speed 16 mm motion pictures. The data from the high speed videography was coupled to a motion analysis software package to calculate shed ice particle size. The potential for future use of these systems on engine inlets will be determined in part by the size, shape, and quantity of the shed ice particles that the engine can safely ingest. The USAF and NASA are exploring this possibility by first identifying whether the information can be captured and credibly measured. This test provides the first opportunity to develop a database that characterizes several of these low power systems.

HARDWARE AND SYSTEM DESCRIPTION

Icing Research Tunnel

The NASA Lewis IRT is a closed-loop refrigerated wind tunnel. A 5000 hp fan provides airspeeds up to 134 m/sec (300 mph). The 21 000 ton capacity refrigeration heat exchanger can control the total temperature from -1.1 to -42°C. The spray nozzles provide droplet sizes from approximately 10 to 40 μm median volume droplet (MVD) diameters with liquid water contents (LWC) ranging from 0.2 to 3.0 g/m^3. The test section of the tunnel is 1.83 m (6 ft) high and 2.74 m (9 ft) wide.

Model Hardware

The testing was done on a 1.83 m (6 ft) span NACA 0012 airfoil with a 0.53 m (21 in.) chord (Figure 1) and a 8.43 mm (0.332 in.) leading edge radius. There was a break between the leading and trailing edges at 0.18 m (7.00 in.) that allowed the front section to be removed. The leading edge was made of fiberglass with three thickness options: 1.52 mm (0.060 in.), 3.17 mm (0.125 in.), and 6.35 mm (0.250 in.). The trailing edge was made with a wood spar, foam core, and a fiberglass skin. The model was mounted vertically in the center of the test section and set at a 4° angle-of-attack for the entire test.

KODAK EKTAPRO 1000 Motion Analyzer

The KODAK EKTAPRO Motion Analyzer consists of an intensified imager, a controller and the EKTAPRO 1000 Processor. The KODAK EKTAPRO 1000 Imager has an image intensifier assembly behind the lens and in front of the sensor which functions as an electronic shutter and light amplifier. This increases the imager's ability to capture events in low light and reduce the blurring of objects moving through the field of view very rapidly. The intensified imager sends its video output to a standard KODAK EKTAPRO 1000 Processor and in addition is connected to a KODAK EKTAPRO Intensified Imager Controller. The gate time (the amount of time the electronic shutter is open during each frame) can be adjusted from 10 μs to 5 msec.

The EKTAPRO 1000 Analyzer, whose resolution is 240 columns of pixels by 192 rows of pixels, provides a video output signal compatible with either NTSC (North American) standard or PAL (European) standard video recording signal formats. The processor is equipped with two video output jacks through which the image from the EKTAPRO 1000 cassette can be copied to a video cassette recorder.

Ice Protection Technologies

The systems tested can be broadly defined under four different technologies: electro-expulsive, eddy current repulsive, high pressure pneumatic-expulsive, and low profile conventional pneumatic. The first two technologies require a capacitor bank storage supply to provide the high amperage, short duration current pulse necessary to initiate the repulsive mechanism. The last two use pneumatic pressure to generate the ice debonding process.

One system used electro-expulsive technology, the Dataproducts New England, Inc. EEDS. The deicer is composed of two conductors overlaying each other in an elastomeric blanket (Figure 2) Reference (1). High amperage, opposing currents are discharged through the conductors (from a capacitor storage supply) with the resulting magnetic fields producing a repulsive force. This causes the upper conductor to be repelled with a high magnitude, short duration force which debonds and expels the ice accreted to the outer elastomer.

A number of systems used eddy current repulsive technology, and they can be divided into two categories. The first group used what is commonly referred to as EIDI coils. They include Rohr Industries, Inc., Advance Concepts De-Icing Company, and Garrett Canada. Each system was designed and fabricated according to specific company desires, but the general repulsive mechanism is the same for all three (Figure 3). A high amperage electric current pulse is sent through a spirally wound cylindrical coil located on the inside of the wing leading edge Reference (2). This produces a magnetic field which induces an eddy current in the doubler plate attached to the outer skin. The two currents' fields repel each other with a resultant small displacement, high acceleration force that cracks and debonds the ice. All three of these systems had a fiberglass outer skin. The second group uses the same electrical phenomena, but their coils are placed on the outside of the airfoil and under an outer skin made of titanium. These include the Electroimpact, Inc. EDS system and the BFGoodrich Company EMS deicer. The two companies use different variations of the same technology to shed ice; only the EDS system will be discussed (Figure 4). As in the case of the EIDI coils, current is passed through the spirally wound pancake coil setting up an eddy current in the doubler Reference (3). The two currents' fields oppose each other resulting in a low displacement, high acceleration movement that breaks the bond between the ice and the outer skin and expels the ice outward.

There was one pneumatic-expulsive technology that used high pressure air to initiate the expelling force. This system was the PIIP deicer tested by BFGoodrich Company. The deicer is composed of a matrix of spanwise fabric-reinforced tubes which lay flat in the relaxed state (Figure 5) Reference (4) . When the system is activated the rapidly pressurized tubes expand slightly with a resultant distortion of the outer surface that debonds the ice. The high acceleration of the skin due to the extremely fast pressure pulse launches the shattered particles into the airstream. For this test the outer skin was made of polyetheretherketone (PEEK).

The final technology tested was a variation on conventional pneumatic deicers, the BFGoodrich Company STP system (Figure 6). This deicer uses relatively low pressure to inflate a number of spanwise tubes embedded in an elastomer blanket, that subsequently break the ice bonds. The aerodynamic forces from tunnel velocity then help to remove the debonded ice and carry it away.

TEST METHODS

Test Conditions

Two different icing conditions were simulated: glaze and rime ice. The airspeed for the glaze ice condition was 67 m/s (150 mph) at -3.9 °C (25°F) with 0.55 g/m^3 of LWC, and 20 µm of MVD. The rime ice condition was at 103 m/s (230 mph), -17.2 °C (1° F), 0.36 g/m^3, and 15 µm. Both conditions fall within calibration settings for the IRT and were chosen from the Federal Aviation Regulations (FAR 25) icing envelope for Continuous Maximum Atmospheric Icing Conditions.

Each system was tested at two different firing modes. For the first firing mode, the icing cloud spray was turned on for a specified time, then turned off, and the system was fired. This firing mode will be referred to as a single event. Seven spray times were used for the single event runs. Those were 1, 2, 4, 6, 8, 12, and 20 minutes. For the other mode, the system was fired at specified intervals during a continuous spray event. This will be referred to as a continuous cycling event. The spray time for this firing mode was fixed at 30 minutes and three different cycling times were used: 1, 3, and 5 minutes. It was necessary to alter the spray time and cycling time for some systems due to differences in design configurations.

Visual Data Acquisition

A KODAK EKTAPRO 1000 high speed video camera system described in the Hardware And System Description section was used to collect information on ice shedding. The field of view was chosen to cover the mid-span of the airfoil where there is good cloud uniformity, and the boot firing characteristics are equivalent for all the systems tested. Resulting dimensions for the field of view were about 0.33 m high (13 in.) and 0.41 m (15 in.) wide. The camera was positioned 1.64 m (64.5 in.) away from the airfoil, shooting perpendicular to the airfoil chordwise axis to minimize the optical distortion due to angularity. After several test runs, it was decided that a recording rate of 1000 frames per second provides nonblurred images to define ice particle edges, as well as enough images to analyze ice particles before they leave the field of view. Although the EKTAPRO system is able to provide nonblurred images at 1000 frames per second under the ambient light condition, it was subjected to high intensity light during the test because of the 16 mm high speed film camera lighting requirements used for the test.

Each recording started just prior to a firing and typically lasted about 2 to 3 seconds for single events. For continuous cycling events, ice shedding was recorded twice during the spray and

the last recording was made after the spray was turned off. All information was stored in specially designed KODAK video tapes to preserve the original resolution for later data reduction. Prior to testing, a grid map was located parallel to the airfoil chordwise axis at several different distances from the airfoil and recorded to provide reference lengths for field of view corrections.

A 16 mm high speed film camera was used as a back-up for the EKTAPRO system. This high speed film camera was mounted horizontally with an angle of approximately 32° to the airfoil chordwise axis to provide a wider field of view than the one the EKTAPRO system provided. The resulting field of view included the whole airfoil chord and about 0.81 m after the trailing edge. The trigger for the camera was tied to the lighting switch so that when the lights were turned on, the camera started recording. The camera was typically run at 3500 frames per second and provided pictures with much higher resolution than the EKTAPRO pictures. Grid map pictures were also taken in the same manner as for the EKTAPRO system.

An electronically gated video camera from Xybion Electronic Systems was mounted on the hatch above the tunnel test section and aimed downward, parallel to the pressure surface of the airfoil. A numbered grid map (0.0254 m squares) on the floor of the test section was included in the field of view so that when ice was expelled outward from the airfoil surface the particle distance could be documented. The images from this camera provided information on how far ice particles travelled away from the airfoil as they were going downstream. This data was used to generate scaling factors to correct the intensified imager field of view information.

A 35 mm camera with a high speed motor drive was mounted above the 16 mm high speed film camera to document ice shedding. The high speed motor drive enabled the camera to take five pictures per second at 1/8000 shutter speed. This provided sharp non-blurred images of ice shedding for some runs. For post-run photographic information, two 35 mm cameras were used to document residual ice shapes and any close-up information on ice formations. These cameras were carried into the tunnel for close-up shots and overall model shots. In addition to the visual equipment described above, a VHS video camera was mounted on the tunnel ceiling upstream of the model to record an overall view of the test for general documentation and tunnel operation monitoring purposes.

Figure 7 shows the set up of all of the control room visual documentation equipment.

Residual Ice Thickness Measurement

After a firing, the tunnel speed was brought down to idle and test personnel went inside the test section to measure residual ice at the leading edge tip and the lower surface (pressure side) at various spanwise locations. The upper surface (suction side) was normally clear, but measurements were made at the upper surface if noticeable residual ice was present. A dial indicator gage with a dial which could read down to 25 μm (1/1000 in.) was modified for this purpose (Figure 8). There were several measurements made before firings to document ice thickness. For these measurements, a hole was made through the ice using a heated rod and the contact arm of the gage was inserted in the hole. Measurement location at the lower surface was determined to be where the thickest ice was found. Spanwise locations of ice left along the leading edge tip, known as cap ice, were also documented.

Ice Shape Tracing

Ice profiles at the mid-span were traced on cardboard templates for ice shape documentation with some systems as test schedules allowed. After the ice accretion was completed for a desired spray time, a heated metal template was pushed into the ice forming a narrow band of uniced surface. A cardboard template was then placed perpendicular to the spanwise direction and the ice shape was traced. Figure 9 shows a metal template placed at the midsection of the model.

Ice Particle Size Measurement

Ice shedding images on EKTAPRO tapes were analyzed to calculate the ice particle size using a program called MOPRO that was modified to map the particle boundary. MOPRO, loaded on a personal computer, can communicate with the EKTAPRO processor through RS-232 or IEEE-488 ports provided on the back of the EKTAPRO processor. Images recorded on EKTAPRO tapes are digitized data and they can be transmitted to a personal computer using MOPRO commands.

A particle is defined by enclosing its boundary using a PC-DOS mouse; then MOPRO counts the number of pixels occupied within the boundary. The pixel count is converted to an area with a physical dimension by applying a scale factor. A scaling factor is necessary to provide image plane depth correction because it was found from the overhead shots that ice particles travel outward from the airfoil as they go downstream. The distance out depended on system, airspeed, and time, so a number of reference lengths were chosen. This scale factor is determined from images of a known grid scale that are specified distances from the airfoil lower surface. The grid scale was suspended parallel to the plane containing the airfoil chordwise axis; the distances were measured at the maximum thickness of the airfoil. The grid, composed of 0.0254 m (1 in.) squares, was displayed in the EKTAPRO camera image plane at four different reference lengths: 0.0254 m (1 in.), 0.127 m (5 in.), 0.254 m (10 in.), and 0.381 m (15 in.). The images were recorded and placed in the EKTAPRO processor nonvolatile memory where they were used to provide the correlation between scale factor and particle distance away from the airfoil.

A typical procedure for ice particle size measurement is as follows. The ice shed event is monitored in a frame by frame sequence until the particle displays the largest frontal area. The boundary of the particle is mapped with a mouse (through MOPRO), then a corresponding overhead shot from the Xybion camera is found to determine the linear distance of the particle from the airfoil surface. This is used to calculate a scaling factor which is applied to the pixel area representing the size of the particle. For each shedding event, size measurements were typically made for the three biggest particles. Figure 10 shows the sequence of a typical ice shedding event.

A limitation was found during the data acquisition using the high speed videography. In some cases, particles from the ice shedding event were carried by the airstream over the upper surface. The amount appeared to increase with spray time, especially for the glaze conditions as the upper surface horn became more pronounced. Due to the time constraints imposed on each test entry there simply was not enough time to move the high speed videography equipment to the opposite side of the tunnel to capture this information. It is hard to gage how much effect, if any, this occurrence had on the database.

Power Monitoring

Power was measured at the line voltage input to each of the power supplies for the capacitor bank storage systems with two separate sets of transducers. The first set contained a current transformer, current transducer, and a voltage transducer. These provided transient information about current and voltage fluctuations. The second set was a current and voltage pick-up that was matched to a wattmeter, providing system power usage in watts. Data was taken at 50, 100, or 500 ms intervals depending on power supply charge rate. The PIIP system power was monitored at the input to the compressor pump. The STP system used high pressure nitrogen bottles as the operating reservoir and NASA did not monitor power for this system.

The number of element firings per deicing event and the power required were left up to the individual participants. Each company was given a check-out period to optimize their deicer settings. All the companies chose to use two firings per deicing event to remove the ice. However, it was found in many cases, especially above 4 minute spray times, that the second discharge was relatively ineffective.

RESULTS

The results presented here do not go into detail on a per system basis. The sheer quantity of data and the sensitivity of certain company specific results dictate that this is not the proper forum to release all this information. The figures included and the general discussion of the data reflect the outcome of the tests.

The icing encounter documentation can be divided into two broad categories. The shed ice particle size is important when examining conditions that are pertinent to engine ice ingestion. The quantity and thickness of ice remaining on a surface have a direct relation to aeroperformance concerns.

Shed Ice Particle Size

The shed ice particles were quantified for 1,2,4,8, and 20 minute spray times only due to the labor intensive task of manually reducing the EKTAPRO data. The particle size data reduced from this test was examined in a number of ways to try and best capture its value in relation to engine ice ingestion parameters. The basic data is shown in Figure 11 and provides a sampling of the three largest particles per run (with a repeat run at each condition) for both the glaze and rime ice conditions. The trend displayed here is common to most of the companies - as the spray time increases the size of the particles gets larger. It was also generally found that the glaze particles were larger than the rime particles for a given spray time. There were not enough repeat runs to provide the data set size necessary to allow a statistical sampling.

The upper bound shed ice values for each of the spray times were used in conjunction with a volume equivalence for 6.35 to 25.4 mm (1/4 to 1 in.) diameter spheres (in 1/4 in. increments) to generate plots that reflect cycling time sensitivity to a specified particle size (Figure 12). The four curves that extend downward from left to right are calculated by dividing a spherical volume by the measured ice thickness for a given spray time. This information reflects a constant thickness area equivalence that might be representative of an engine ice ingestion tolerance curve. Plotted against these curves are the upper bound area values for specific spray times. The intersection of this curve with the family of constant thickness area equivalence curves provides an indication of the cycling times required to stay within a specified ice sphere envelope. For example, in Figure 12(b), the upper bound area curve intersects the 1/2" sphere curve at just under 4 min. This would be the longest cycling time, between deicer boot firings, allowable to maintain particle sizes under a 1/2" sphere volume equivalence. Engine tolerance limits may be sensitive to ice particle shape, but as an initial cut, this format appears to provide useful information for engine inlet deicing analysis.

Residual Ice Thickness

Residual ice was documented at the leading edge, at the lower surface (pressure side), and at the upper surface (suction side). Cap ice along the span was also documented. Each deicer had different residual ice characteristics due to differences in system design. For this reason, measurement locations along the span varied for the systems. The device and techniques used for

these measurements were described in the Hardware and System Description section, and the Test Methods section.

All systems tested generally cleaned the leading edge fairly well for all spray times for both glaze and rime ice conditions. However, all systems left ice at the lower surface and, with a few systems, ridges of thin ice were observed at the upper surface.

Since all EIDI systems had coils at the mid-span and the PIIP, STP and EEDS systems do not have spanwise variations on performance due to their design configurations, the characteristics of the residual ice at the mid-span location were considered to be most representative in terms of the ice removing capability of the systems. Also, ice accretion was believed to be most representative for the given cloud conditions at the mid-span because the cloud uniformity was considered to be best there.

Figure 13 is an example of the plots of residual ice thickness at the mid-span for glaze and rime ice. The reader should be reminded that these plots do not represent the typical range or the behavior of the residual ice thickness for all the systems tested. Thickness of residual ice at the lower surface generally grew with the spray time, until it either reached a plateau or started decreasing. It appears reasonable that thickness grows with the spray time since there would have been thicker ice to clear for the longer spray. An explanation is not available at this time as to why the thickness begins decreasing at longer spray times with some systems.

Ice thickness measured from the actual ice tracings at the leading edge and at the lower surface for the range of spray times are shown in Figures14 and 15 to provide some references on the thickness of the ice build-up. The ice tracings were made before the systems were activated. All thicknesses are averaged values from several systems with which the ice tracings were made. The ice thickness for the 20 minute spray was extrapolated from the measured thicknesses. The range of residual ice thickness at the lower surface at the mid-span spreads from less than 0.25 mm (0.010 in.) to 4.45 mm (0.175 in.) for all the spray times tested.

Power

The capacitor bank power supply systems that were used in six of the eight systems were "lab" or test equipment and were not optimized for a specific application. The power data that was recorded during the test was reported in watts, a common method used in thermal system inforamtion, i.e., power densities (watts/area). However, upon examination, this turns out to be a very misrepresentative number for a generic test such as this. Both the charge time and the number of unit element firings per deicing event have a direct bearing on a final watt density value, and are configuration specific. Since charge time will be dependent on the number of elements per power supply, cycling times per element, airfoil contamination requirements, etc., it should not be included in this kind of test. This has led to the use of energy values - both in energy/unit element (Joules) and energy density (Joules/area). For the six companies, the energy settings to fire an element once ranged from approximately 250 to 1050 Joules. The values were set at the beginning of the test and remained constant throughout (some companies did change energy settings from glaze to rime ice). When the data was normalized to energy/unit area, two trends became noticeable: (1) the three EIDI systems had very similar values - approximately 0.5 to 0.6 Joules/cm^2 (3 to 4 Joules/in.^{2}), and (2) the remaining three systems were also grouped together but at a higher value - approximately 1.7 to 2 Joules/cm^2 (11 to 13 Joules/in^2). The PIIP system compressor power was reported in watts, and, as stated earlier, no power information was monitored on the STP deicer.

CONCLUSIONS

The test was the first of its kind in terms of testing several new ice protection technologies under identical icing conditions. As a result, an extensive database for residual ice, particle size, and power information has been assembled. One of the outcomes of the test has been the development of a set of test techniques including a methodology that allows the capture and analytical post-test processing of ice shedding events.

It became apparent during the high speed videography analysis that an image processing technique with an automated pattern recognition capability would provide considerably more information and the potential for defining mass distribution data on the shed ice. This would possibly supply the range of shed ice information necessary to identify a system's applicability to an engine inlet. This new technique is currently being examined.

ACKNOWLEDGEMENTS

It took the efforts of a number of different disciplines to make this test a success. The authors wish to thank all those involved throughout the development of this project, in particular the NASA Lewis Imaging Science Group, the IRT Test Installations Division personnel, the Model Development Branch, and the IRT Aeropropulsion Facilities and Experiments Division personnel.

REFERENCES

1. Golberg, J. and Lardiere, B., "Developments in Explusive Separation Ice Protection Blankets," AIAA Paper 89-0774, Jan. 1989.

2. Zumwalt, G.W., Schrag, R.L., Bernhart, W.D., and Friedberg, R.A., "Electro-Impulse De-IcingTesting Analysis and Design," NASA CR-4175, Setp. 1988.
3. Smith, S.O. and Zieve, P.B., "Thin Film Eddy Current Impulse Deicer," AIAA Paper 90-0761, Jan. 1990.

ORIGINAL PAGE
BLACK AND WHITE PHOTOGRAPH

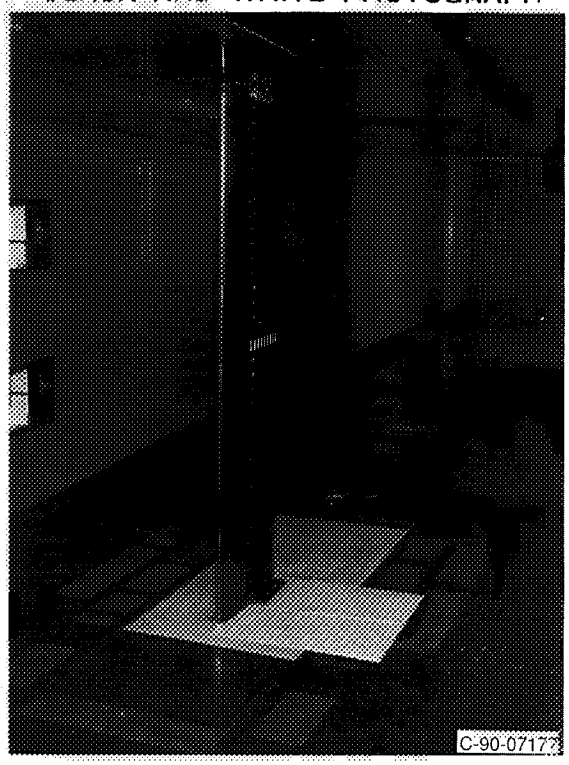

Figure 1.—NACA 0012 airfoil with low power deicer in the IRT.

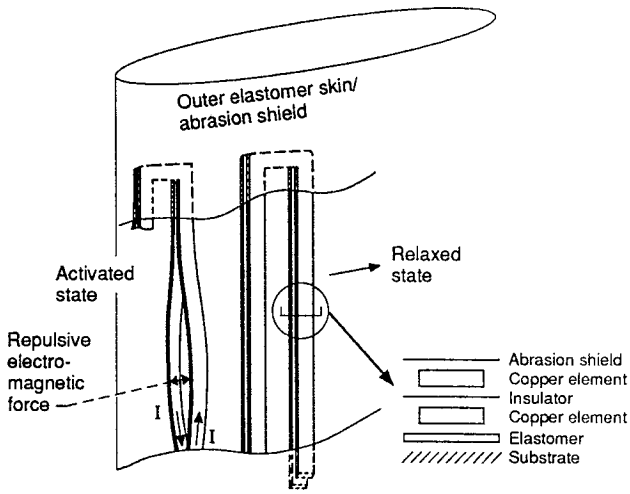

Figure 2.—Dataproducts New England, Inc. Electro-Expulsive Deicing System schematic.

4. Martin, C. and Putt, J., "An Advanced Pneumatic Impulse Ice Protection System (PIIP) for Aircraft," AIAA Paper 90-0492, Jan. 1990.

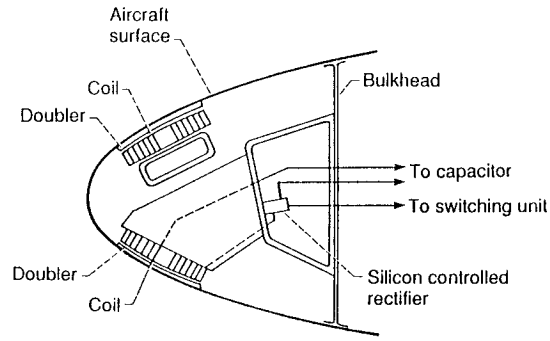

Figure 3.—Electro-Impulse Deicing Coil.

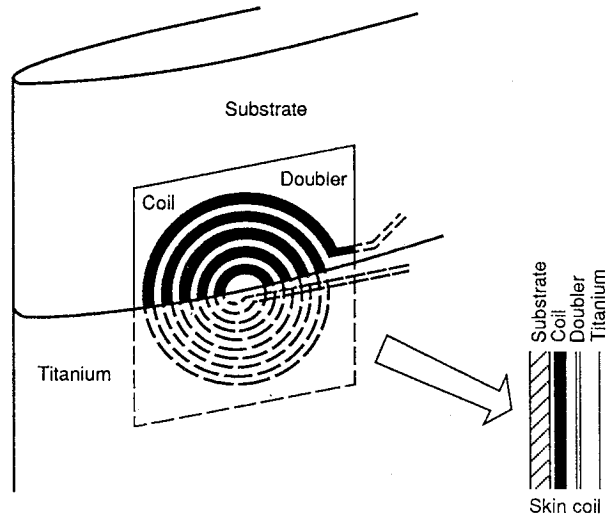

Figure 4.—Electroimpact, Inc. Eddy Current Repulsion Deicing Strip.

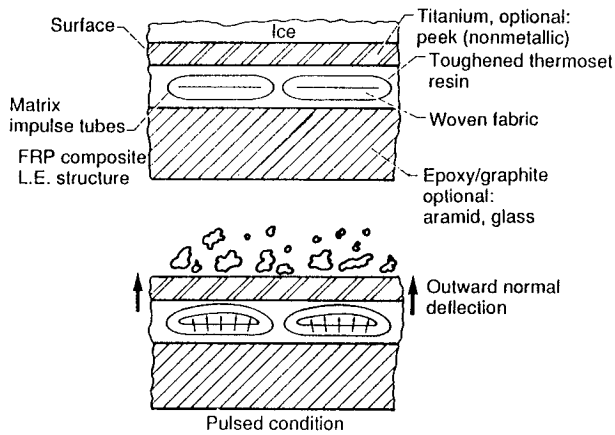

Figure 5.—B. F. Goodrich De-Icing Systems Pneumatic Impulse Ice Protection system schematic.

ORIGINAL PAGE
BLACK AND WHITE PHOTOGRAPH

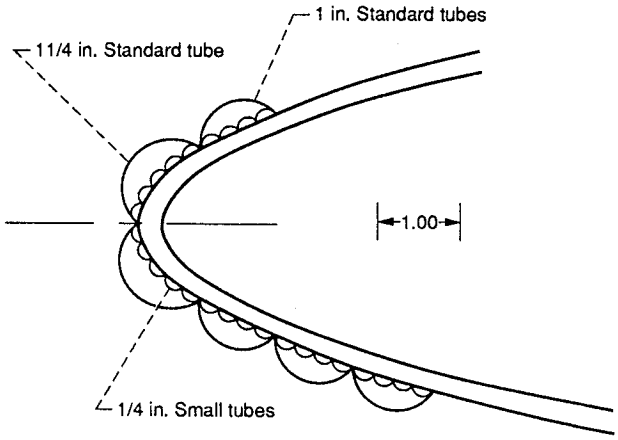

Figure 6.—B. F. Goodrich De-Icing Systems Small Tube Pneumatic system.

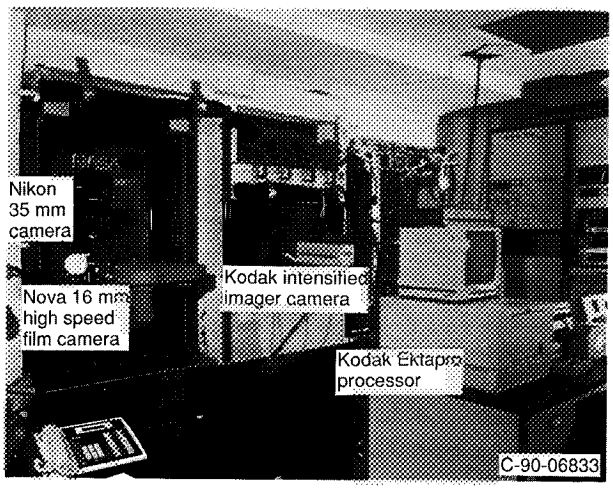

Figure 7.—Imaging equipment in the IRT control room.

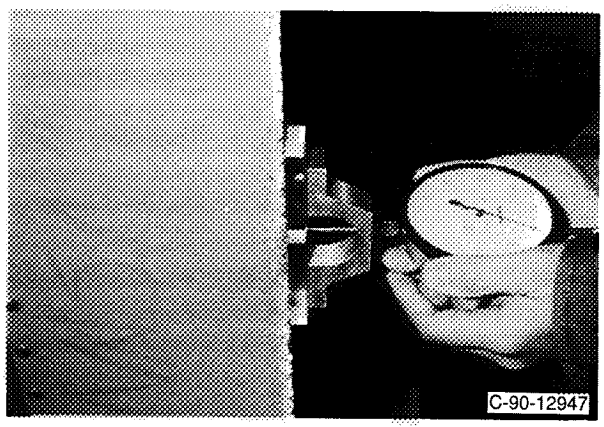

Figure 8.—Leading edge ice thickness measurement.

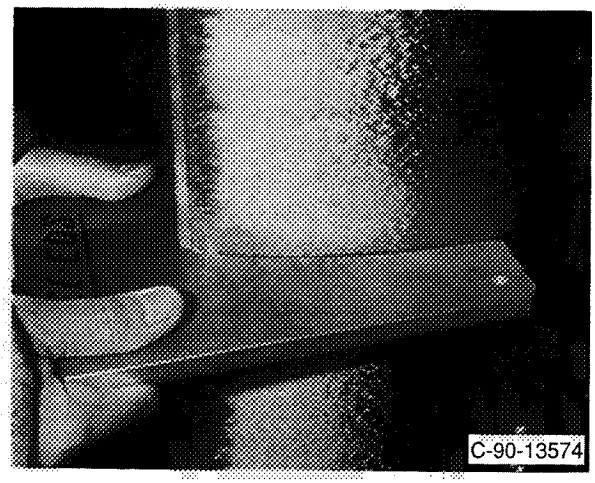

Figure 9.—Metal template melting ice accretion for profile trace.

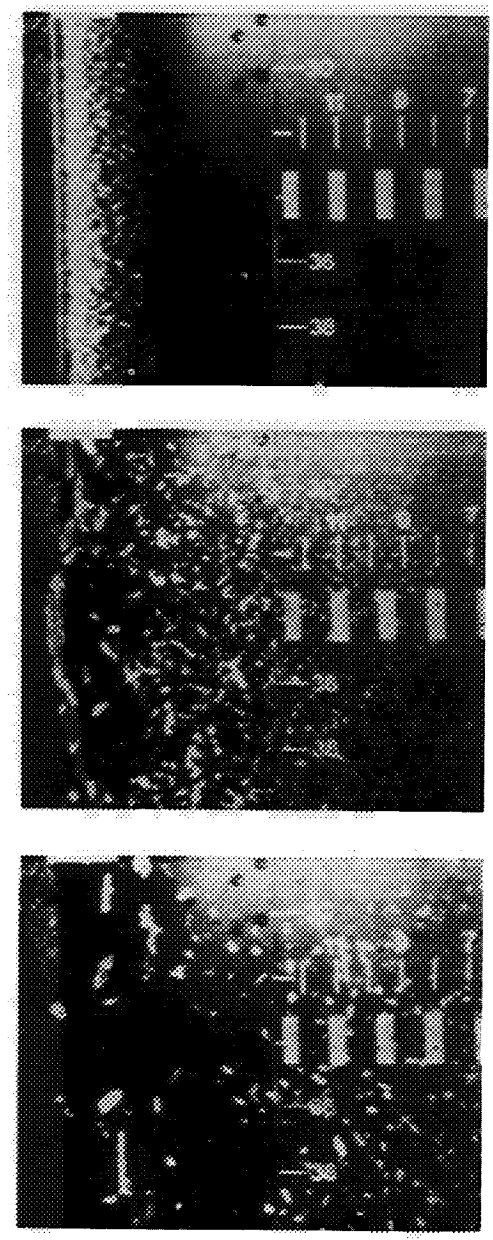

Figure 10.—Ice shedding sequence from low power ice protection system. High speed videography to capture ice shedding event; 6 minute spray-glaze ice.

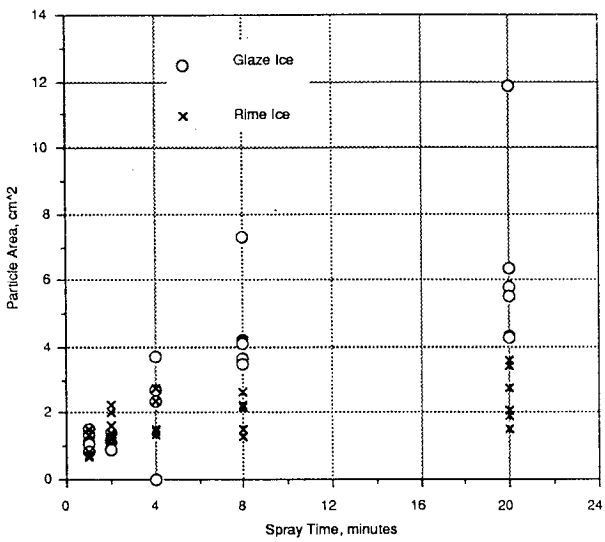

Figure 11.—Shed ice particle size as measured by high speed videography system.

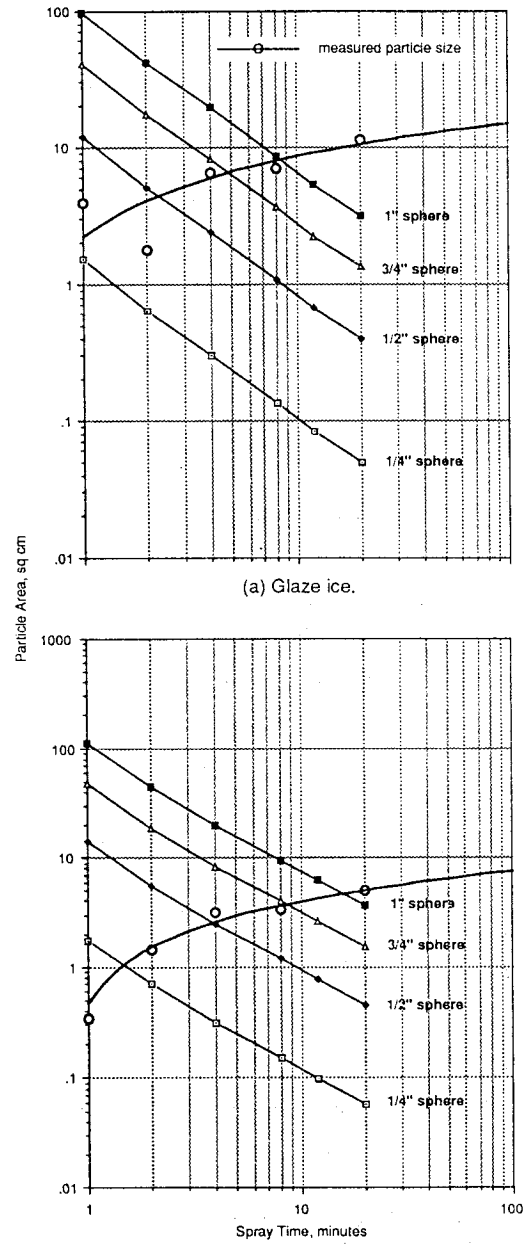

(a) Glaze ice.

(b) Rime ice.

Figure 12.—Area equivalence for shed ice particles. Labeled sphere curves are area equivalence based on spherical volume divided by measured ice thickness for specific spray times. Thickness taken at leading edge.

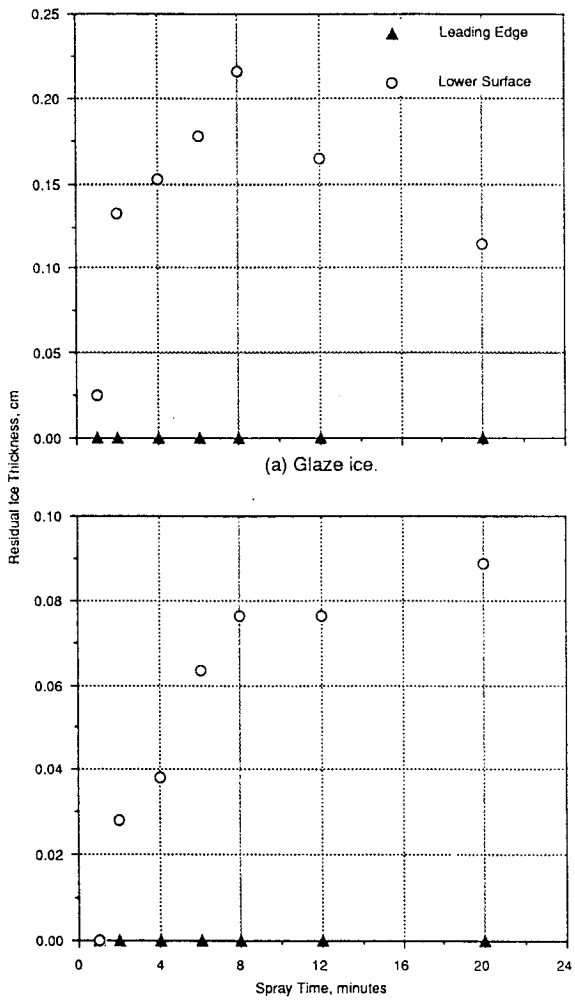

(a) Glaze ice.

(b) Rime ice.

Figure 13.—Residual ice thickness on NACA 0012 airfoil, taken at the mid-span position.

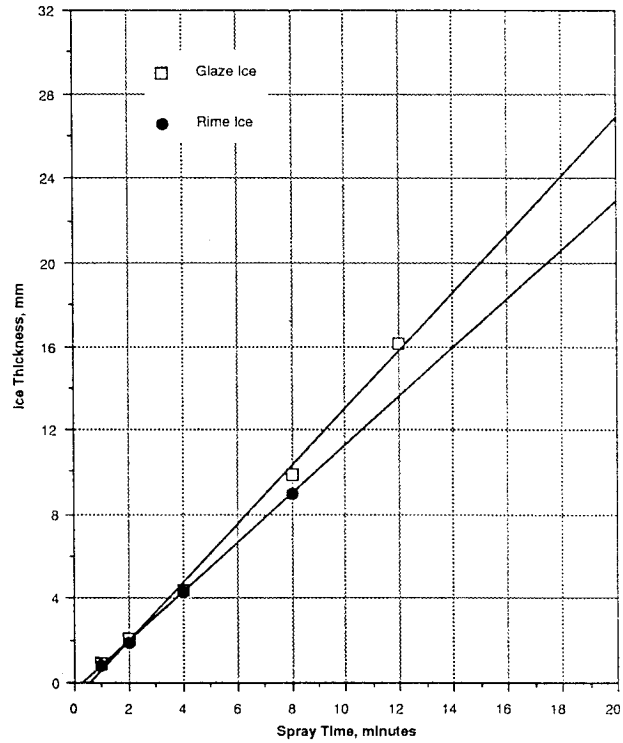

Figure 14.—Measured ice thickness at the leading edge; averaged from several measurements taken at the mid-span.

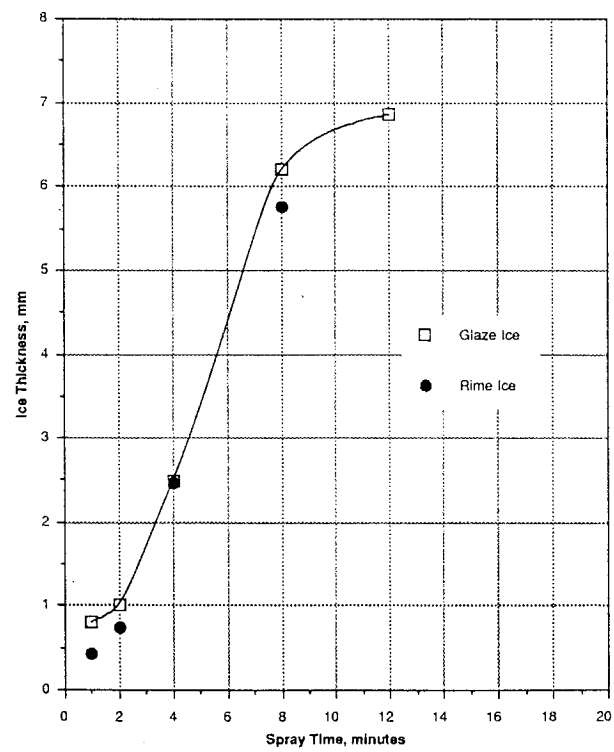

Figure 15.—Measured ice thickness at the lower surface; averaged from several measurements taken at the mid-span.

NASA
National Aeronautics and Space Administration

Report Documentation Page

1. Report No. NASA TM-103757	2. Government Accession No.	3. Recipient's Catalog No.
4. Title and Subtitle Advanced Ice Protection Systems Test in the NASA Lewis Icing Research Tunnel		5. Report Date
		6. Performing Organization Code
7. Author(s) Thomas H. Bond, Jaiwon Shin, and Geert A. Mesander		8. Performing Organization Report No. E-6013
		10. Work Unit No. 505-68-11
9. Performing Organization Name and Address National Aeronautics and Space Administration Lewis Research Center Cleveland, Ohio 44135-3191		11. Contract or Grant No.
		13. Type of Report and Period Covered Technical Memorandum
12. Sponsoring Agency Name and Address National Aeronautics and Space Administration Washington, D.C. 20546-0001		14. Sponsoring Agency Code

15. Supplementary Notes

Prepared for the 47th Annual Forum and Technology Display sponsored by the American Helicopter Society, Phoenix, Arizona, May 6-8, 1991. Thomas H. Bond and Jaiwon Shin, NASA Lewis Research Center. Geert A. Mesander, United States Air Force, Oklahoma City Air Logistics Center, Tinker Air Force Base, Oklahoma. Responsible person, Thomas H. Bond, (216) 433-3414.

16. Abstract

Tests of eight different deicing systems based on variations of three different technologies were conducted in the NASA Lewis Research Center Icing Research Tunnel in June and July of 1990. Six companies participated in this joint United States Air Force/NASA ice protection technology program. The deicing systems used pneumatic, eddy current repulsive, and electro-expulsive means to shed ice. The tests were conducted on a 1.83 m (6 ft) span, 0.53 m (21 in.) chord NACA 0012 airfoil operated at a 4° angle-of-attack. The models were tested at two temperatures: a glaze condition at −3.9 °C and a rime condition at −17.2 °C. The systems were tested through a range of icing spray times and cycling rates. Characterization of the deicers was accomplished by monitoring power consumption, ice shed particle size, and residual ice. High speed video motion analysis was performed to quantify ice particle size.

17. Key Words (Suggested by Author(s)) Icing tunnel tests Advanced deicer systems	18. Distribution Statement Unclassified−Unlimited Subject Category 07

19. Security Classif. (of this report)	20. Security Classif. (of this page)	21. No. of pages	22. Price*
Unclassified	Unclassified	12	A03

NASA FORM 1626 OCT 86 *For sale by the National Technical Information Service, Springfield, Virginia 22161

PAGE 1 INTENTIONALLY BLANK

PRECEDING PAGE BLANK NOT FILMED